PUBLICATIONS OF THE ASTRONOMICAL SOCIETY OF THE PACIFIC, 112:97–107, 2000 January

Why Adaptive Secondaries?

J. H. LEE

Satellite Technology Research Center, Korea Advanced Institute of Science and Technology, 373-1 Kusong-dong, Yusong-gu, Taejon 305-701, Republic of Korea; jhl@satrec.kaist.ac.kr

B. C. BIGELOW

The Observatories of the Carnegie Institution of Washington, 813 Santa Barbara Street, Pasadena, CA 91101

AND

D. D. WALKER, A. P. DOEL, AND R. G. BINGHAM

Optical Science Laboratory, Department of Physics and Astronomy, University College London, University of London, Gower Street, London WC1E 6BT, England, UK

Received 1999 May 23; accepted 1999 September 7

ABSTRACT. Adaptive optics (AO) combines technologies that enable the correction in real time of the wavefront distortion caused by the terrestrial atmospheric turbulence. An adaptive secondary mirror (ASM), unlike conventional adaptive optics systems, does not add any polarization, reflective losses, and emissivity.

Following successful implementation of tip/tilt secondary mirrors, most recent large telescope projects have considered the possibility of incorporating ASMs. This paper briefly reviews the development of ASMs and examines the issues which have arisen and also presents the predicted performance of an ASM system. It is concluded that adaptive secondary approach is an equally satisfactory or preferred solution to conventional AO systems.

1. INTRODUCTION

Adaptive optics (AO) systems remove the wavefront distortion introduced by the Earth's atmosphere (or other turbulent medium) by means of an optical component(s) introducing a controllable counterwavefront distortion which both spatially and temporally follows that of the atmosphere Beckers (1993). Telescope adaptive secondary mirrors (ASMs) (Fig. 1), which use an existing optical surface (the secondary mirror) as the wavefront corrector, were proposed by Beckers (1989) to improve the performance of an adaptive optics system by elimination of the extra optical surfaces found in conventional AO systems.

This paper examines general issues concerning the development of the ASMs, which include the performance comparison between a conventional system and an ASM. This paper also presents the developments of ASMs and the predicted performance for adaptive secondaries based on simulation and experimental results.

2. PERFORMANCE COMPARISON

Conventional AO systems operate like auxiliary instruments and are more or less independent of the telescope. A typical system uses additional relay optics to form an image of the telescope's pupil or an image conjugated with a nominal turbulent layer(s) in the atmosphere on a deformable(s) mounted on an optical bench. The system usually also includes a separate mirror for removing the tip/tilt component of the wavefront distortion. Further reimaging optics are then required to bring the light to a focus on the science and wavefront sensing camera.

Since an ASM approach needs no extra relay or reimaging optics, the approach has several advantages compared to the conventional approach: (1) optical throughput is greatly enhanced; (2) negligible extra infrared emissivity is introduced, which is a crucial advantage for a system intended to operate primarily in the infrared; and (3) no extra polarization is caused.

This section presents the results of a comparison analysis between a generic ASM as shown in Figure 1 and a preliminary design for a conventional AO system for the William Herschel Telescope (WHT; Longmore 1997; M. Wells 1999, private communication) which gives a measure of the performance of the systems in terms of throughput, emissivity, and polarization. The respective minimum numbers of surfaces for the two systems, excluding the telescope primary and secondary mirrors, are tabulated in Table 1. The ASM is assumed to use a Shack-Hartmann wavefront sensor (WFS) with an array of small lenslets, which adds two extra

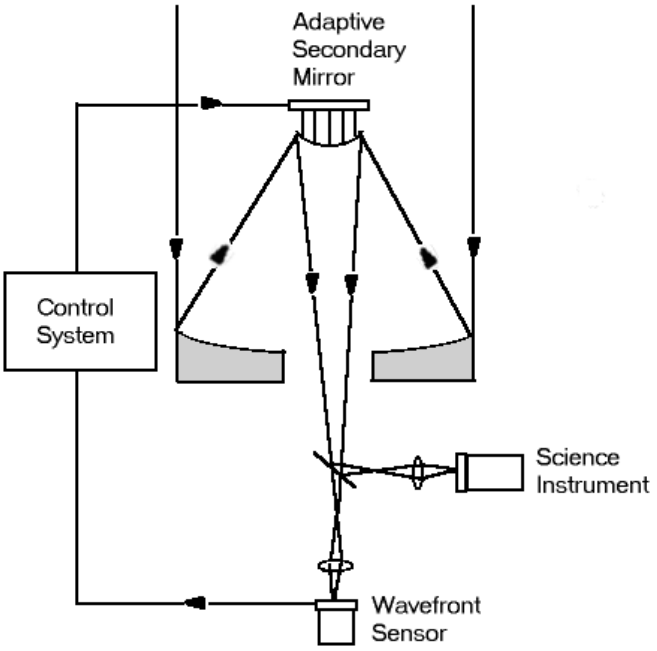

FIG. 1.—Schematic diagram of an ASM system

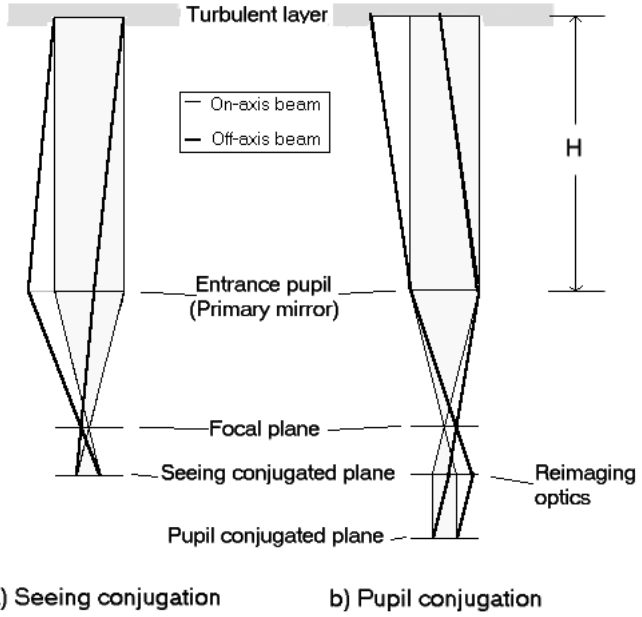

FIG. 3.—Schematic diagram of (*a*) seeing conjugation and (*b*) pupil conjugation.

refractive surfaces to the WFS optical beam than the science optical path.

2.1. Throughput

Throughput is a measure of the proportion of light that is transmitted through an optical system. Many AO systems employ a polychromatic approach in which the wavefront sensing is performed in a different spectral band from that used for the scientific observation. The observation is usually made in the infrared band while the light in the visible band is used for the wavefront sensing. Therefore the throughputs in both bands are important.

A comparison of throughput is given below, based simply on the number of optical surfaces in the different systems. All the reflective and refractive surfaces were assumed to be coated by overcoated silver and broadband multilayer anti-

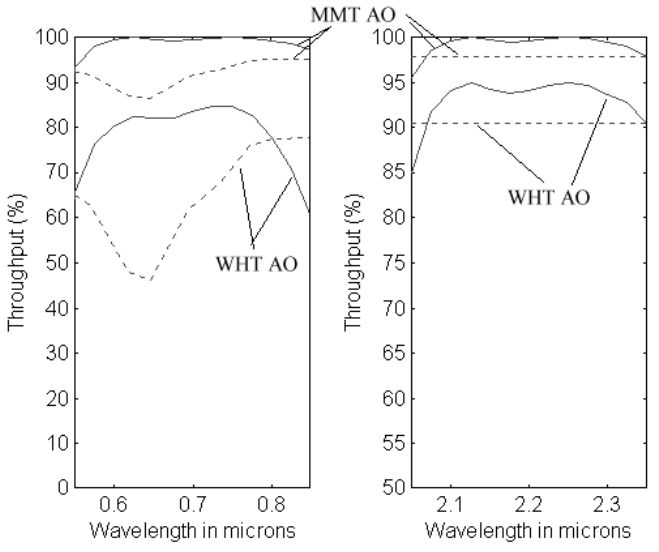

FIG. 2.—Total throughput (%) for the conventional system and ASM (*a*) for wavefront sensing (centered at 0.7 μm) and (*b*) for the science instrument (centered at 2.2 μm).

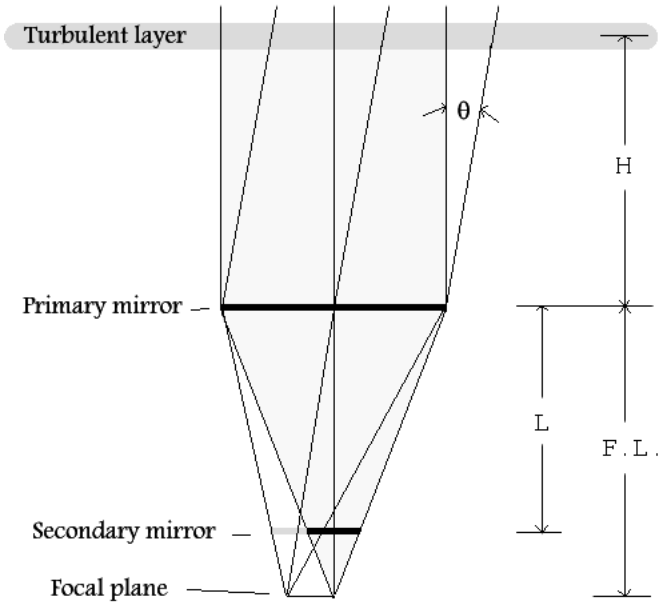

FIG. 4.—Pupil conjugation with shear and vignetting at the (Cassegrain) secondary mirror.

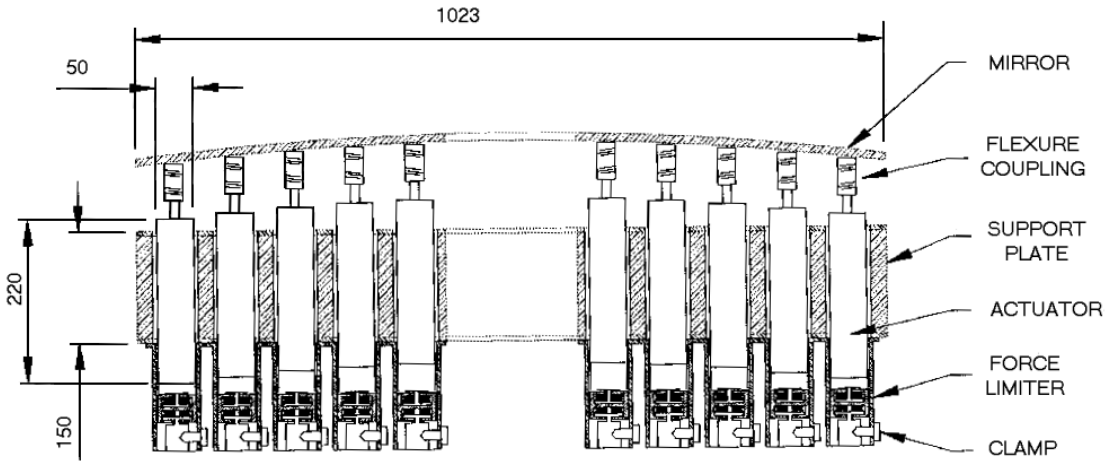

FIG. 5.—Schematic of a 1 m deformable ASM with 90 actuators

reflection coatings, respectively. The data on the reflectivity of these coatings are widely available (Ealing Electro-optics Inc.). Normal incidence for refraction was assumed for simplicity, as departure from normal incidence only marginally effects the resulting values.

TABLE 1

REFLECTING AND REFRACTING SURFACES COUNTS FOR A CONVENTIONAL (WHT) SYSTEM AND AN ASM AO SYSTEM

Optical Path	Reflections	Refractions	Total Surfaces
WHT Nasmyth System			
WFS.....	7	9	16
Science	5	5	10
MMT Adaptive Secondary			
WFS.....	...	4	4
Science	...	2	2

The total throughputs (Fig. 2) for both cases were calculated assuming a polychromatic wavefront sensing system. The wavelength ranges for antireflection coatings were assumed to be centered at 0.7 and 2.2 μm for the wavefront sensing and the science instrument, respectively. Note the different Y-axis (the total throughput) scales.

The conventional system will lose 17% and 6% of the original flux to the wavefront sensor and to the science instrument, respectively. In contrast, the ASM will lose less than 1% of the original flux in both cases. For the same total flux in the wavefront sensor, the conventional system requires a 20% brighter guide star to compensate for a 17% loss of the original flux. As the coatings deteriorate with time, the difference between the total losses will be larger and so will the difference between the limiting stellar magnitudes for the conventional and ASM systems. For example, when the original reflectivity has deteriorated by 4%, the total losses will become 60% for the conventional system and 12% for the ASM system. The additional loss in the

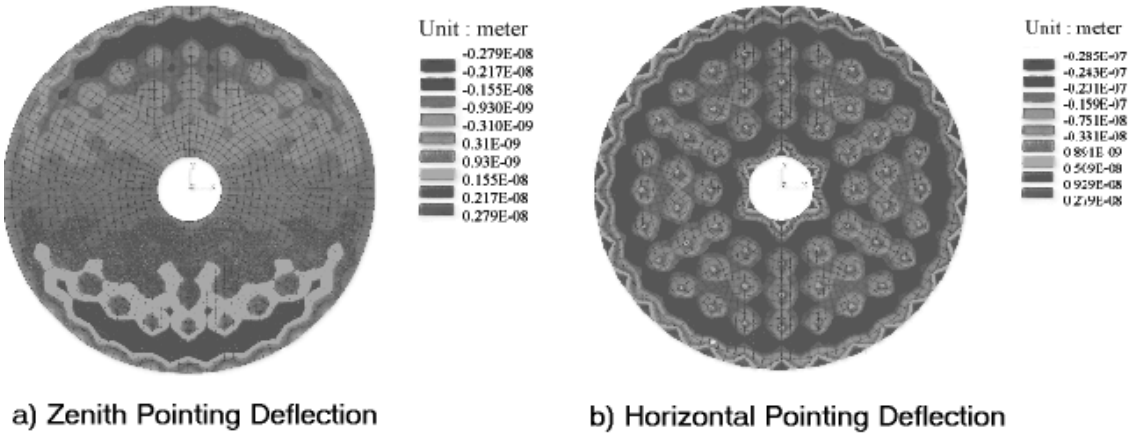

FIG. 6.—Static deflection of the mirror substrate under gravity

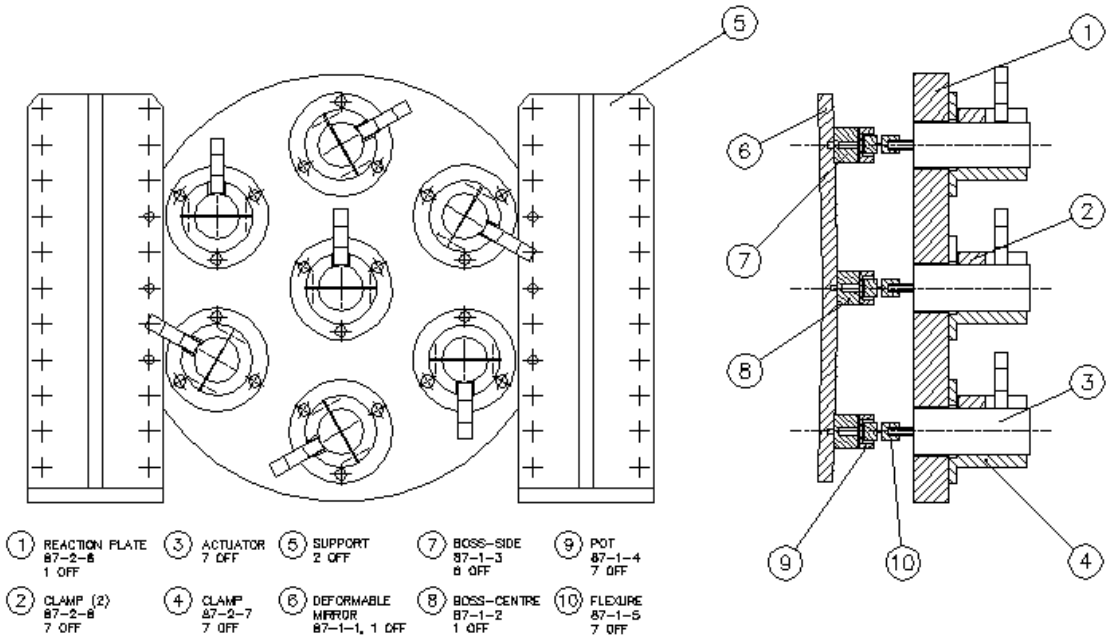

FIG. 7.—Mechanical design of the demonstrator

conventional system then requires an increase in integration times by a factor of 2.5, even if background noise has not become significant.

The required magnitude for the natural guide star is determined by many factors including the level of adaptive compensation, the telescope aperture, and the readout noise and spectral response of the WFS detector. However, the loss of 1 stellar magnitude will significantly reduce the number of astronomical objects accessible to the AO system and hence the science instrument it feeds.

2.2. Emissivity

For infrared observations, emissivity in the optical train will reduce the signal-to-noise ratio of the data. A detailed comparison of emissivity is currently not possible because such an analysis requires detailed information about the AO system optics, temperature, baffling, and the surrounding environment, none of which is available. However, an approximate comparison can be made, again based on the number of optical surfaces in the system and emissivity of each optical surface.

Dinger (1993) assumed a mirror emissivity of 0.0076 in his thermal emissivity analysis of the Gemini telescope. Assuming the optical surfaces in the two AO systems have the same emissivity of the Gemini mirror, the total emissivity, including the effects of the primary and secondary mirror, for the conventional and ASM AO are 8.04% and 3.04%, respectively. The total emissivity for the ASM AO is approximately 2.5 times smaller than that of the conventional system. The difference is more likely to be greater in a real case since refractive surfaces usually have a significantly higher emissivity than reflective surfaces.

The comparison shows that a conventional post-Cassegrain or Nasmyth-focus AO system significantly degrades the telescope emissivity. A low infrared emissivity is a crucial advantage for a system with strong science drivers in the infrared.

2.3. Polarization

Polarization yields information about asymmetry inherent in the astrophysical environments, which may be within the source itself, or in the medium between source and observer, or both (Tinbergen 1996). Polarization is often a good way of obtaining otherwise inaccessible information about the internal structure of the source and, in particular, magnetic fields and the effects of dust and scattering. In many astronomically interesting cases, polarization of less than 1% may be astrophysically interesting.

The science optical path of the conventional system contains eight reflections including an extra three reflections for the Nasmyth image derotator, while the ASM AO science optical path contains two refractions. The ASM system is assumed to operate at Cassegrain focus but not at Nasmyth focus (in which case an ASM would need a derotator). The polarization of the conventional system was calculated just from the angles of incidence at the mirrors, which were 60°, 30°, 60°, 16°9, 14°, 7°, 45°, and 69° along the optical path. The calculation assumed all optical surfaces were silver coated.

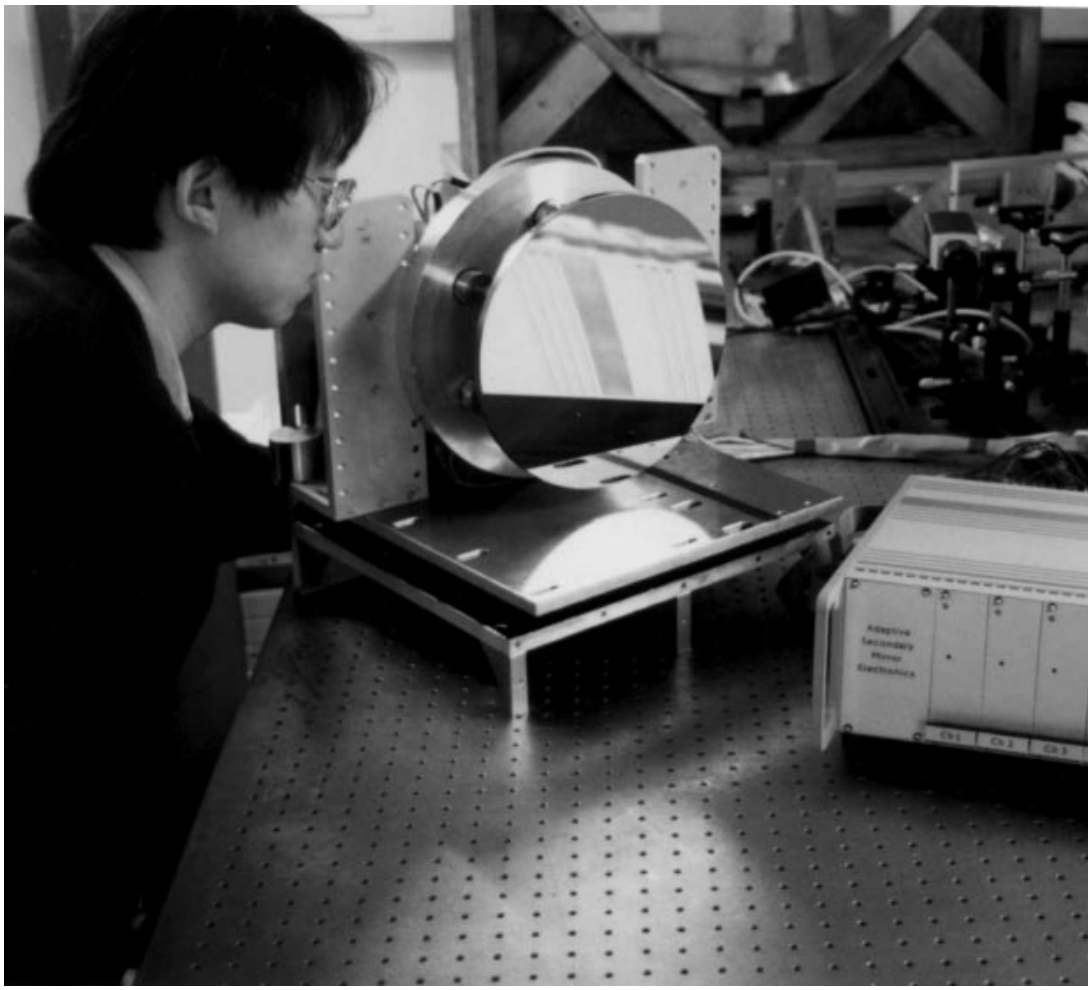

FIG. 8.—Demonstrator unit after assembly

Considering only reflections, the conventional system would have total $R_{\perp}$ of 0.8450 and $R_{\parallel}$ of 0.9145, where $R_{\perp}$ and $R_{\parallel}$ are intensity reflection coefficients for perpendicular and parallel components of the electromagnetic light vector. The resultant polarization of the conventional system would be 1.98% while the ASM system would have no extra polarization.

Therefore conventional systems can introduce significant polarization. This can be greatly reduced if the systems are designed to have low incidence angles ($<10°$), although this is often difficult to achieve on an operational telescope due to space restrictions. However, even if a conventional AO system is designed with very careful selection of materials and angles of incidence, such a system creates difficulties for making high-sensitivity ($<0.1\%$) polarization measurements. This is because the polarization introduced may depend on the orientation of the telescope.

2.4. Applications using Coronagraphy

Stray light arises from both scattering and specular reflections at lens surfaces. Although the amount of scattered and other stray light in an optical system depends strongly on its actual design, the fewer optical surfaces in an ASM system and especially the elimination of lenses will always lead to lower stray light levels. This will have particular relevance in imaging or spectroscopy of faint structure near bright sources using coronagraphy, where the stray light is of crucial importance. For coronagraphy in the near-infrared, for example, of protoplanetary disks and brown dwarfs companions, the reduced infrared emissivity of an ASM will also be a significant advantage.

3. LOCATION OF AN ASM AS A WAVEFRONT CORRECTOR

In conventional AO systems, there are mainly two types of conjugation of a deformable mirror(s) as shown in Figure 3. In pupil conjugation, the correcting mirror is effectively conjugated to the telescope pupil. Wavefronts from both the on-axis and off-axis wavefronts almost completely illumi-

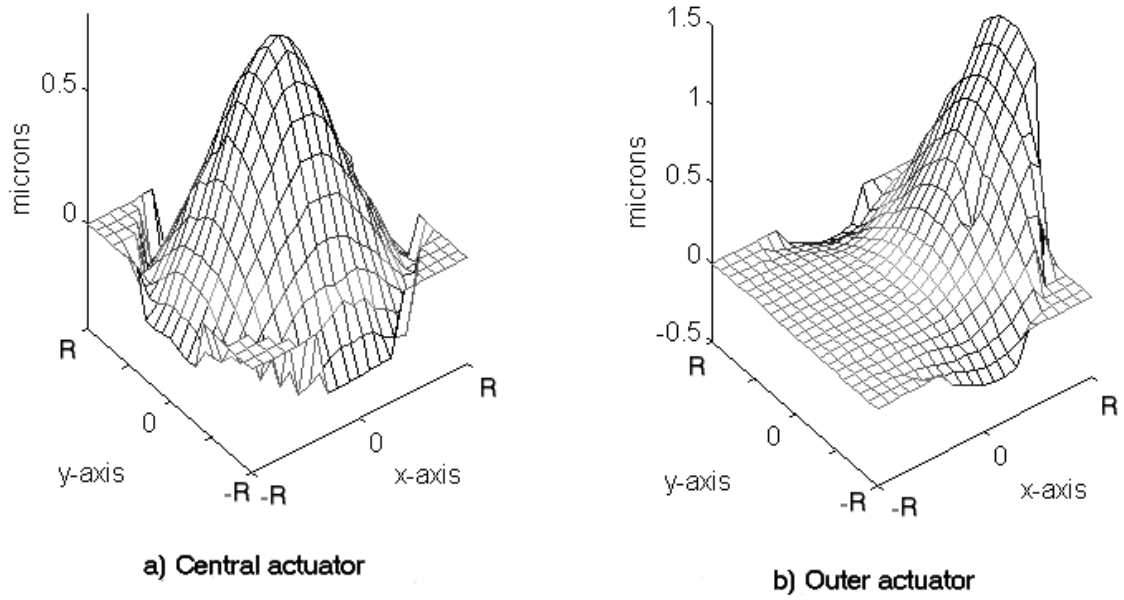

FIG. 9.—Influence functions of central and outer actuators of the demonstrator. R on X- and Y-axes is the radius of the mirror.

nate the primary mirror (no vignetting), but follow slightly different paths through the atmosphere and a shear $S = \theta H$ occurs between the two wavefronts, where q is the angular separation between the two wavefronts in radians and H is the altitude of the (assumed) single layer of turbulence.

Seeing conjugation refers to locating the correcting mirror(s) at the conjugate to the layer(s) of turbulence at a given altitude. Roddier (1981) shows that locating the wavefront corrector at the conjugate to the turbulent layer has the potential to improve the isoplanatic angle by as much as a factor of 2. In this case, the on-axis and off-axis wavefronts pass through the same phase screen (no shear), but part of the off-axis wavefront is lost at the primary mirror (vignetting).

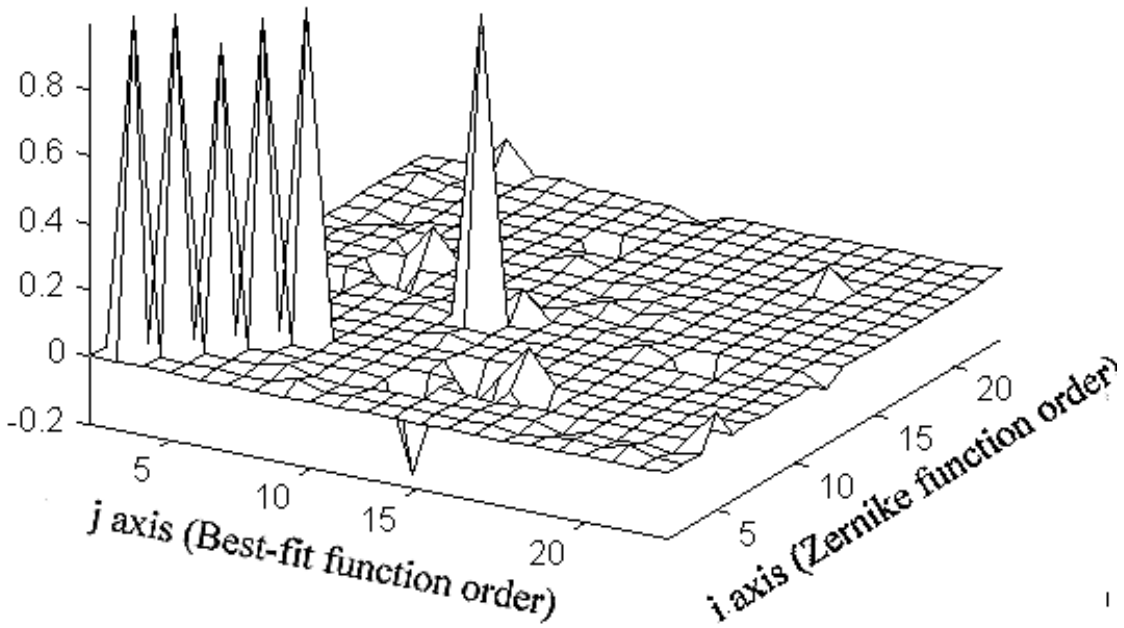

FIG. 10.—Ability of the 27 cm demonstrator to fit Zernike terms. See the Appendix.

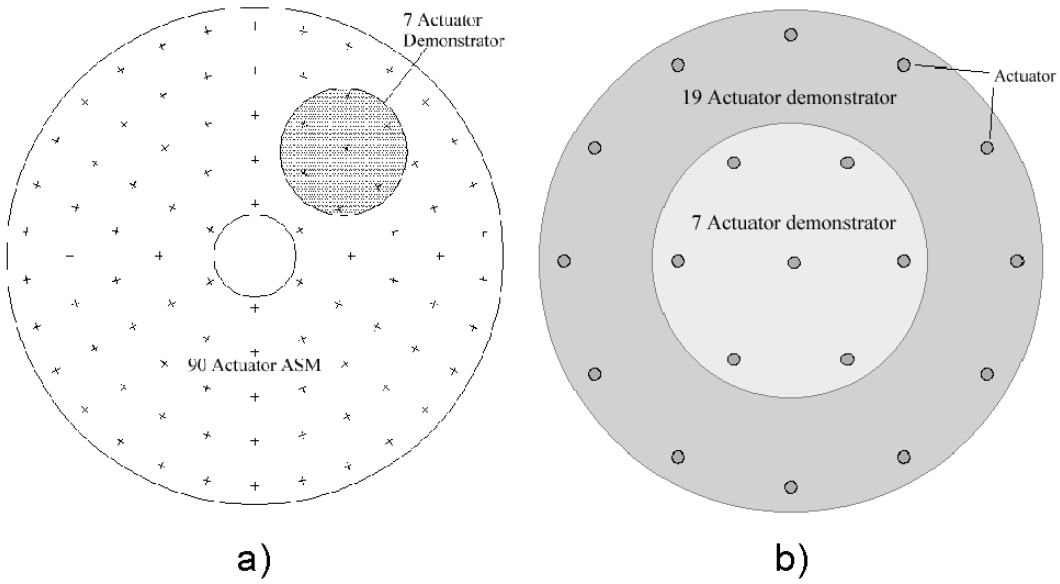

FIG. 11.—(*a*) Drawing of a 1 m mirror with 90 actuators positioned at plus marks in the drawing. Small circle represents the demonstrator of 27 cm with seven actuators. (*b*) Inside and outside circles represent the demonstrator with seven and 19 actuators, respectively.

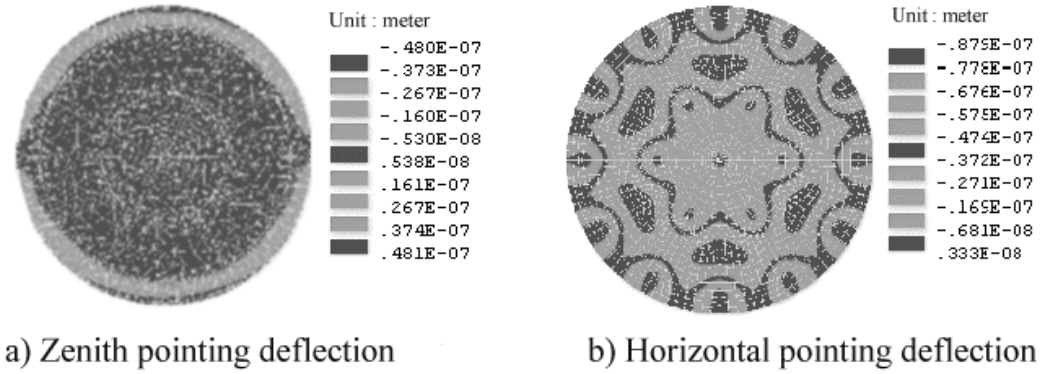

FIG. 12.—Static deflection of the 60 cm demonstrator under gravity

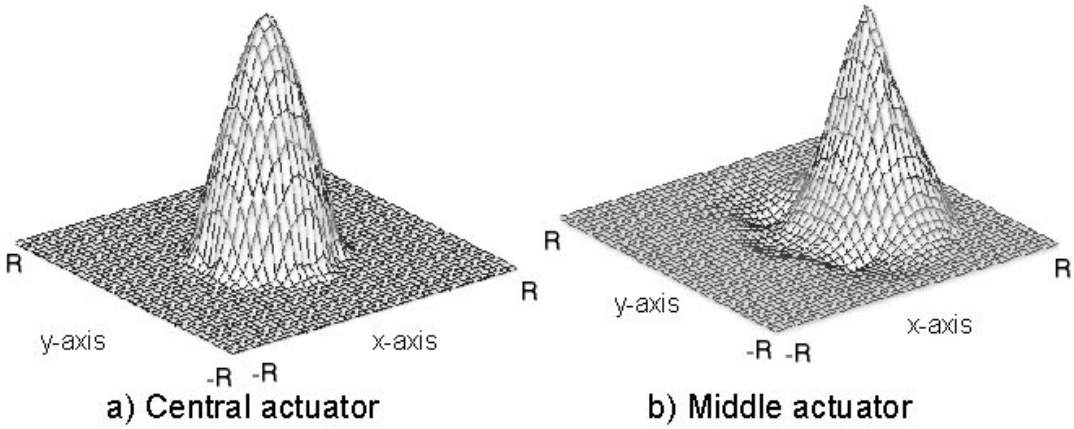

FIG. 13.—Influence functions of the actuators of the 60 cm demonstrator. *R* on *X*- and *Y*-axes is the radius of the mirror.

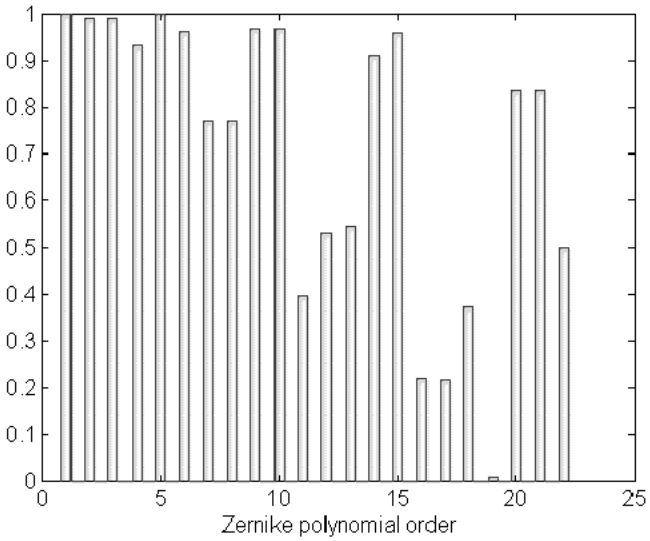

FIG. 14.—Ability of the 60 cm demonstrator to fit Zernike terms. See the Appendix.

In the case of an ASM, the mirror is not conjugate to any atmospheric turbulent layer but to some distance below or above the telescope depending on the type of telescope: Cassegrain or Gregorian. Adaptive correction with the secondary mirror contains features of both types of conjugation: shearing and vignetting.

As shown in Figure 4 the on-axis and off-axis wavefronts will be sheared at the secondary, and part of the off-axis wavefront will be lost. The magnitude of the shear will be qL, where L is the primary/secondary separation and q is the angular distance between on-axis and off-axis wavefronts in radians. As an example, on UKIRT, for which a deformable ASM mirror has been proposed, for an angular separation of 60″, the shear will be approximately 2.5 mm. The UKIRT f/35 secondary is roughly 316 mm in diameter, and the portion of the wavefront lost is simply the total area minus the geometric overlap of the two wavefronts. The fractional area lost $\mathrm{FA}_{\mathrm{lost}}$ is then

$$\mathrm{FA}_{\mathrm{lost}} = 1 - \frac{2}{\pi}\cos^{-1}\left(\frac{S}{2R}\right) + \frac{S}{\pi R^2}\sqrt{R^2 - \frac{S^2}{4}}, \qquad (1)$$

where S is the size of shear and R is the radius of the secondary mirror. For $S = 2.5$ mm and $R = 158$ mm, the fraction lost is 0.01, or only 1% of the off-axis wavefront. The corresponding values for Gemini and a 60″ off-axis angle lead to a shear of 3.6 mm and a fractional area loss of 0.3%. The effect is negligible.

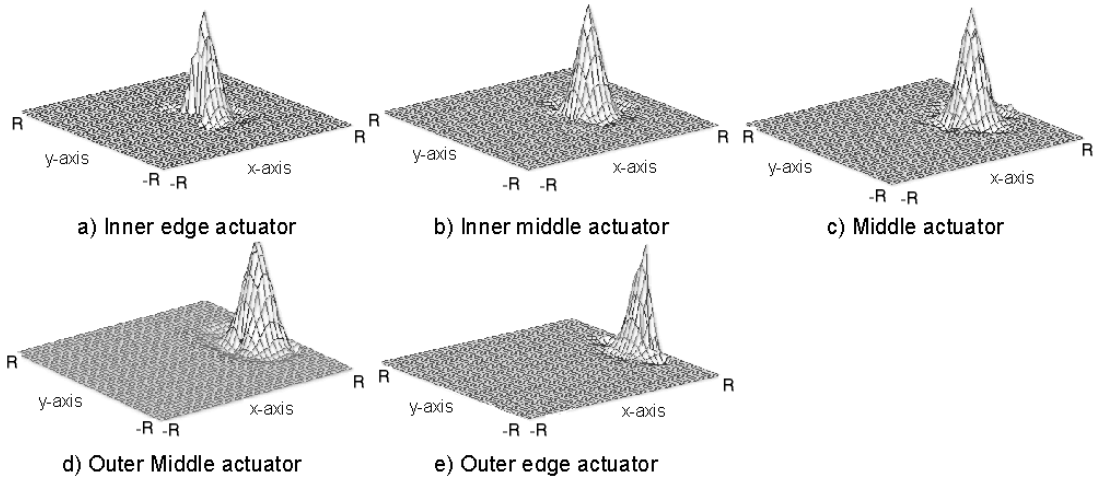

FIG. 15.—Influence functions of the 1 m ASM. R on X- and Y-axes is the radius of the mirror.

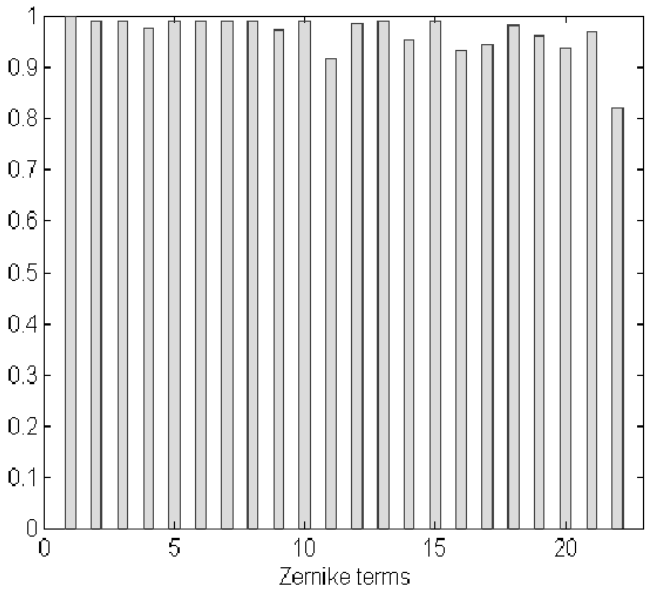

FIG. 16.—Ability of the 1 m ASM to fit Zernike terms. See the Appendix.

In 1993, J. M. Hill[1] pointed out that a Gregorian ASM has some advantages to a Cassegrain configuration. A ellipsoidal Gregorian secondary allows access to the prime focus for artificial stars or wavefront sensors to measure the primary or secondary surface independently. The concave adaptive secondary can be easily tested because it forms images at real and accessible conjugates, which allows the adaptive secondary to be calibrated or monitored independently from the primary and/or without a reference star. This is one of reasons why the Optical Science Laboratory (OSL) demonstrator mirror (Lee, Walker, & Doel 1999a, 1999b) and the prototypes of the Multiple-Mirror Telescope (MMT) AO (Salinari & Sander 1998) were chosen to be concave rather than convex.

In addition to this, a Gregorian secondary would be conjugate to a height in the atmosphere a few hundreds meters above the telescope. While this has the potential to increase the effective isoplanatic angle if the dominant seeing layer is situated close to this height, this is unlikely in practice to be the case. A Gregorian telescope still has disadvantages compared to a Cassegrain configuration: (1) increase in telescope length necessitating an increase in the size of the dome; (2) the diameter of a Gregorian secondary is larger than that of a Cassegrain, so increasing central obstruction and increasing the inertia of the secondary mirror, which might reduce tip/tilt and chopping performance.

As previously commented, the secondary mirror is conjugated to some distance below or above the telescope. This will have the effect of reducing the isoplanatic field to compared to a traditional, aperture-conjugated system. The sky coverage of an ASM system could, however, be increased by shifting the compensation correction calculated from the wavefront sensor data prior to application to the deformable secondary, as proposed by Walker, Bingham, & Biglow (1993).

4. SYSTEM DESIRABILITY FOR ASMs

An ASM is an integral part of the telescope rather than an independent auxiliary instrument. Therefore, the ASM telescope as a system will fail if the ASM control fails. More seriously, when near zenith pointing, the secondary mirror is directly over the telescope primary, which is therefore vulnerable to any catastrophic stress-induced fracture of the secondary. Therefore, an ASM should use reliable and nonfragile materials and components. This is particularly the case for the mirror blank but also includes other components such as the actuators. Certain elements of the control system (particular power supplies, power drivers) may usefully be duplicated to provide redundancy, if this can be made consistent with the allowable mass and mass-moment budgets.

There is also a very strong pointer toward incorporating a switch-off mode so that the secondary will still provide scientifically useful imaging (even if degraded and/or for use only in the infrared) in the event of a complete control-system failure. In service the stresses applied to the mirror area small are compared to the yield strength of the material. Therefore even in the case of a partial failure (e.g., one actuator goes to maximum extent), the mirror substrate

[1] J. M. Hill, The Gregorian Question, Technical Memorandum UA-93-02, is located at http://medusa.as.arizona.edu/lbtwww/tech/ua9302.htm.

will not be distorted to an extent that would cause the material to behave inelastically.

5. CURRENT STATUS OF THE DEVELOPMENT OF ASMs

Close & McCarthy (1994) have demonstrated a tip/tilt secondary mirror on the Steward Observatory 2.3 m telescope. This system makes use of a 6.5 inch diameter secondary mirror which is driven by three actuators. A similar system has been operated on the University of Hawaii 2.2 m telescope (Young & Cavedoni 1993). Another tip/tilt secondary mirror has been built for the UK Infrared Telescope 3.8 m telescope in a collaboration between the Royal Observatory Edinburgh and the Max-Plank-Institute für Astronomic Heidelberg (Pitz, Rohloff, & Marth 1993). In the sense that compensation of only tip/tilt does not constitute fully adaptive correction, these secondary mirrors are not ASMs. However, the successful implementation of these tip/tilt secondary mirrors has shown that high temporal frequency correction can be applied at the secondary mirror and even this limited implementation is useful.

At present, there is no operating large telescope utilizing a deformable secondary mirror. However, prototype ASMs have been developed at the Steward Observatory in collaboration with several other partners and independently at the OSL at University College London. The Steward Observatory is developing a 0.65 m deformable ASM prototype with 320 actuators (Bruns, Barrett, & Sandler 1996) and has built some smaller prototypes to investigate system performance (Salinari & Sander 1998). The Steward system is designed for operation from the visible to the near-infrared. The OSL program is focused on a 1 m deformable ASM with at least 90 actuators and has built and tested a 27 cm mirror to demonstrate the technology (Lee, Walker, & Doel 1999a, 1999b). This system is designed primarily to operate in the near-infrared.

6. PERFORMANCE EXPECTATION

The OSL initially proposed a 1 m ASM with 90 actuators for 8 m class telescopes such as Gemini as shown in Figure 5. The mechanical feasibility of the design was proven by finite-element analysis (FEA). Figure 6 shows that the expected static deflection of the mirror substrate of the design under gravity is smaller than 28.5 nm. This means that the design can provide a static mirror shape to within about $\lambda/20$ at 0.55 μm and $\lambda/80$ at 2.2 μm (peak-to-valley number).

A 27 cm demonstrator with seven actuators, which is essentially a subsection of the 1 m design as shown in Figure 11, was developed in order to explore features and capabilities applicable to a large adaptive secondary mirror and to explore manufacturing, assembly/disassembly, calibration, and measurement techniques (Figs. 7 and 8).

The previous papers (Lee, Walker, & Doel 1999a, 1999b) reported that the demonstrator can fit near-perfect tip/tilt with some other lower other Zernike terms, which was predicted by simulation and proven by experiments. Figures 9 and 10 show the influence functions of the central and outer actuators of the demonstrator and its ability to fit low-order Zernike terms. During the previous studies, we also developed techniques to assemble/disassemble the mirror substrate without disturbing the optical quality of the mirror surface at the level of 10 nm rms. The previous results prove the two fundamental requirements of the adaptive secondaries: (i) the ability of preserving the optical quality of the aluminum mirror during assembly/disassembly and (ii) the ability of deforming the mirror shape as wanted.

Now we are designing a middle-sized demonstrator of 60 cm with 19 actuators (Fig. 11). This new demonstrator program would develop features which are directly applicable to a large secondary and finally would prove this approach before building a real full-sized telescope system.

Figure 12 shows the FEA-derived static deflection of the mirror substrate of the 60 cm demonstrator under gravity. This figure shows that the design has sufficient number of actuators to keep static deformation within 90 nm. Figure 13 shows the influence functions of the central, middle, and outer edge actuators derived by FEA analysis. The comparison of the influence functions of the two demonstrators (Figs. 9 and 13) shows similarity between the two designs as shown in Figure 11. Using these influence functions, the ability of the 60 cm demonstrator to fit Zernike terms (derived as described by Lee, Walker, & Doel 1999a) was shown in Figure 14. This figure shows this demonstrator can correct quite well for the lower order ($Z < 10$) and some higher order Zernike terms.

The 1 m ASM with 90 actuators was simulated in the same manner. Figure 15 shows the influence functions of the actuators of the 1 m ASM, and Figure 16 shows the ability of the 1 m ASM to fit Zernike terms. The analysis was restricted to the first 22 Zernike terms because of processing limitations. This figure shows as expected the 90 actuator ASM can fit all these Zernike terms well. Moreover, considering the numerical errors caused by finite modeling of the mirror during simulation, the predicted performance of the 1 m ASM should be slightly better than that shown in Figure 16.

7. CONCLUSION

Over recent decades telescopes have evolved from massive, passively supported mirrors through to actively driven thin meniscus mirrors. The successful implementation of tip/tilt mirrors on large telescopes has proven the

feasibility of providing high-frequency correction at the secondary mirror. ASMs are the natural next step in the development of telescopes. Significant considerations include throughput, polarization, infrared emissivity, stray light, conjugation, reliability, and predicted performance of ASMs. This paper shows that an ASM is highly attractive in all respects.

The work described in this paper has been financed from a number of sources, including the Satellite Technology Research Center (SaTReC) of the Korea Advanced Institute of Science and Technology (KAIST), the UK Gemini project office, and the UK Particle Physics and Astronomy Research Council.

APPENDIX

DERIVATION OF THE EXPECTED PERFORMANCE

This appendix, which is part of a previously published paper by the authors (Lee, Walker, & Doel 1999a), describes how the expected performance of the deformable mirrors is derived.

The orthogonality α_n between the nth Zernike term Z_n and corresponding mirror's best-fit shape $\mathscr{Z}_n$ is defined by

$$\alpha_n = \int_0^1 r\,dr \int_0^{2\pi} d\theta W(r) Z_n \mathscr{Z}_n\,, \tag{A1}$$

where the weighting function $W(r)$ defining a unit circular aperture is given by

$$W(r) = \begin{cases} \dfrac{1}{\pi} & r \le 1 \\ 0 & r > 1\,. \end{cases} \tag{A2}$$

The mean square fitting error (e^2) for the nth unit-magnitude Zernike term can be written as

$$e^2 = \int_0^1 r\,dr \int_0^{2\pi} d\theta W(r)(Z_n - \mathscr{Z}_n)^2 \simeq 1 - \alpha_n\,. \tag{A3}$$

A value of 1 of α_n means perfect matching while 0 means perfect orthogonality or zero ability to fit the term as shown in equation (A3). The scale of the vertical axis of Figures 10, 14, and 16 represents the value α_n of each deformable mirror.

REFERENCES

Beckers, J. M. 1993, ARA&A, 31, 13
———. 1989, The NOAO 8-M Telescope Technical Description, Vol. 2 (Tucson: NOAO)
Bruns, D. G., Barrett, T. K., & Sandler, D. G. 1997, Proc. SPIE, 2871, 890
Close, L. M., & McCarthy, D. W. 1994, PASP, 106, 77
Dinger, A. S. 1993, Proc. SPIE, 1753, 183
Lee, J. H., Walker D. D., & Doel A. P. 1999a, Opt. Eng., 38(9), 1456
———. 1999b, Opt. Eng., in press
Longmore, A. J., et al. 1997, Proc. Opt. Eng. Soc., 3126
Pitz, E., Rohloff, R. R., & Marth, H. 1993, ICO-16 Satellite Conference on Active and Adaptive Optics (Garching: ESO)
Roddier, F. 1981, Prog. Opt., 19, 281
Salinari, P., & Sandler, D. G. 1998, Proc. SPIE, 3353, 742
Tinbergen, J. 1996, Astronomical Polarimetry (Cambridge: Cambridge Univ. Press)
Walker, D. D., Bingham, R. G., & Biglow, B. C. 1993, in ESO Proc. 48 (Garching: ESO), 253
Young T. T., & Cavedoni C. P. 1993, IOC-16 Satellite Conference on Active and Adaptive Optics (Garching: ESO)